Available online at www.sciencedirect.com
SCIENCE DIRECT
Applied Catalysis A: General 281 (2005) 207–213
APPLIED CATALYSIS A: GENERAL
www.elsevier.com/locate/apcata

Highly active and selective AlSBA-15 catalysts for the vapor phase *tert*-butylation of phenol

A. Vinu[a], Biju M. Devassy[b], S.B. Halligudi[b], Winfried Böhlmann[c], Martin Hartmann[a,*]

[a]*Department of Chemistry, Chemical Technology, Kaiserslautern University of Technology, P.O. Box 3049, D-67653, Kaiserslautern, Germany*
[b]*Inorganic Chemistry and Catalysis Division, National Chemical Laboratory, Pune 411008, India*
[c]*Department of Physics and Geosciences, University of Leipzig, Linnéstr. 5, 04103, Germany*

Received 10 August 2004; received in revised form 23 November 2004; accepted 24 November 2004
Available online 29 December 2004

Abstract

Hexagonally ordered mesoporous AlSBA-15 catalysts having n_{Si}/n_{Al} ratios from 7 to 215 have been synthesized hydrothermally using a cheap non-ionic block copolymer as the structure-directing agent. The obtained materials were analyzed by XRD and nitrogen adsorption to determine the structural order and the textural properties. It has been observed by ^{27}Al MAS NMR spectroscopy that aluminum atoms are exclusively in tetrahedral coordination for all samples except AlSBA-15(7), where octahedral aluminum has been detected to some extent. Temperature-programmed desorption of pyridine showed that AlSBA-15(45) has a higher number of strong acid sites as compared to other mesoporous materials such as FeMCM-41, AlMCM-41 and FeAlMCM-41. The catalyst AlSBA-15(45) showed superior performance in the acid-catalyzed tertiary butylation of phenol employing *tert*-butanol as the alkylation agent. A high phenol conversion of 86.3% is observed for this catalyst at a reaction temperature of 150 °C. Over AlSBA-15(45), the 4-TBP yield amounts to 40.5% and the 2,4-DTBP yield corresponds to 37.9%.

Keywords: SBA-15; Aluminum incorporation; AlSBA-15; Butylation of phenol; Acidity

1. Introduction

Mesoporous molecular sieves have attracted much attention owing to their potential use as versatile catalysts and adsorbents for bulky molecules [1,2]. These materials contain a regular arrangement of uniform channels with diameters between 2 and 10 nm, high specific surface area and high specific pore volume. However, as compared with conventional zeolite catalyst, these materials possess lower acidity (i.e. acid site strength) and hydrothermal stability. Moreover, the thermal and hydrothermal stability is even lower after the introduction of heteroelements such as aluminum and titanium [3,4].

A highly ordered large pore mesoporous silica molecular sieve SBA-15 has been recently synthesized using an amphiphilic triblock copolymer as the structure directing agent in highly acidic media [5–7]. SBA-15 possesses considerably thicker pore walls as compared to MCM-41 and, thus, exhibits significantly higher hydrothermal stability than the latter material [1,6]. Several studies, dealing with the incorporation of Al, V and Ti into SBA-15 by direct synthesis or post synthetic grafting method [8–13] to create active sites in these materials, have been published. During catalyst preparation via post synthetic methods metal oxides are often formed in the channels or on the external surface. Metal oxides formed in the mesopores will block the pores partially or fully thereby reducing surface area, pore volume and pore diameter or will play a negative role in catalysis [14]. Yue et al. [8] have reported the direct synthesis of AlSBA-15 ($n_{Si}/n_{Al} = 10$) and found that the catalytic activity of AlSBA-15 in cumene cracking is higher as compared to AlMCM-41 with a similar n_{Si}/n_{Al} ratio. However, the highly acidic synthesis gel required for the formation of SBA-15 hinders the direct incorporation of high amounts of trivalent metal ions into the neutral silica

* Corresponding author. Tel.: +49 631 205 3559; fax: +49 631 205 4193.
E-mail address: hartmann@rhrk.uni-kl.de (M. Hartmann).

0926-860X/$ – see front matter © 2004 Elsevier B.V. All rights reserved.
doi:10.1016/j.apcata.2004.11.031

framework and a post-synthetic treatment to remove octahedral aluminum is required [8]. Recently, we have reported an optimized procedure for the synthesis of AlSBA-15 [15].

Alkylation of phenol is an industrially important reaction because many alkylated phenols are important intermediates for the manufacture of antioxidants, ultraviolet absorbers, phenolic resins, polymerization inhibitors, lube additives and heat stabilizers for polymeric materials [16]. The alkylation of phenol with *tert*-butanol has been intensively studied in the presence of different catalysts such as aluminum chloride, phosphoric acid, sulfuric acid, silica-alumina, cation exchange resins and microporous molecular sieves [17–26]. *tert*-Butyl derivatives of phenol are precursors for a number of commercially important antioxidants and intermediates in the synthesis of various agrochemicals, flagrances, thermoresistant polymers and protecting agents for plastics [16]. 4-*tert*-Butylphenol (4-TBP) imparts improved performance properties to the class of metallic detergents (phenates) used in lubricating oils whereas 2,4-di-*tert*-butylphenol (2,4-DTBP) is mainly used in the manufacture of its triphosphite which is employed as co-stabilizer for polyvinyl chloride. The major drawbacks of homogeneous catalysts employed in this reaction are their hazardous nature and the required separation of the catalyst from the reaction mixture. On the other hand, cationic exchange resins cannot be used because of their low stability at higher temperature as well as their low activity and selectivity [18,19]. The possible reaction products of the tertiary butylation of phenol depend upon the nature and strength of active sites present in the catalyst [27]. Selvam and co-workers [27–29] have reported the *tert*-butylation of phenol over AlMCM-41 and FeMCM-41 and proposed that the moderate acidity of these catalysts is favorable for the formation of the para-isomer (4-TBP). Very recently, we have reported the *tert*-butylation of phenol over FeAlMCM-41 and FeSBA-1, which exhibit higher conversion and selectivity to 4-TBP as compared with other mesoporous catalysts [30].

In this paper, we report the results of *tert*-butylation of phenol over the large pore mesoporous molecular sieves AlSBA-15 with pore diameters between 9 and 12 nm. AlSBA-15 was synthesized with various n_{Si}/n_{Al} ratios and characterized by XRD, N_2 adsorption and ^{27}Al MAS NMR spectroscopy and its catalytic activity was tested in the *tert*-butylation of phenol. The selectivity to the more bulky 2,4-di-*tert*-butylphenol ($S = 43.9\%$ at 150 °C) is significantly higher as compared to other mesoporous molecular sieves.

2. Experimental

2.1. Materials

Aluminum isopropoxide was obtained from Merck, while tetraethyl orthosilicate and the tri-block copolymer poly(ethylene glycol)-*block*-poly(propylene glycol)-*block*-poly(ethylene glycol) (Pluronic P123, molecular weight = 5800, $EO_{20}PO_{70}EO_{20}$) were obtained from Aldrich.

2.1.1. Synthesis of AlSBA-15

AlSBA-15 was synthesized using Pluronic P123 as the structure-directing agent, as described in our previous paper [15]. In a typical synthesis, 4 g of Pluronic P123 were added to 30 ml of water. After stirring for a few hours, a clear solution was obtained. Thereafter, 70 g of a 0.28 M hydrochloric acid solution were added and the gel was stirred for another 2 h. Then, 9 g of tetraethyl orthosilicate and the required amount of the Al source were added and the resulting mixture was stirred for 24 h at 40 °C The samples were denoted as AlSBA-15(y) where y denotes the n_{Si}/n_{Al} molar ratio. The solid product was recovered by filtration, washed several times with water, and dried overnight at 100 °C. The molar composition of the gel was 1 TEOS:0.02–0.15 Al_2O_3:0.016 P123:0.46 HCl:190 H_2O. Finally, the product was calcined at 540 °C to remove the template.

2.2. Characterization

The powder X-ray diffraction patterns of AlSBA-15 were collected on a Siemens D5005 diffractometer using Cu Kα ($\lambda = 0.154$ nm) radiation. The diffractograms were recorded in the 2θ range of 0.8–10° with a 2θ step size of 0.01° and a step time of 10 s. Nitrogen adsorption and desorption isotherms were recorded at 77 K (−196 °C) on a Quantachrome Autosorb 1 sorption analyzer. All samples were outgassed for 3 h at 250 °C under vacuum ($P < 10^{-5}$ hPa) in the degas port of the sorption analyzer. The specific surface area was calculated using the BET model. The pore size distributions were obtained from the adsorption branch of the nitrogen isotherms using the Barrett–Joyner–Halenda method.

Solid-state ^{27}Al MAS NMR spectra were recorded at room temperature on a Bruker MSL 500 NMR spectrometer at a resonance frequency of 130.32 MHz, applying a short 2.1 μs RF pulse and a recycle delay of 100 ms. The samples were spun at a frequency of about 10 kHz using a 4 mm diameter zirconia rotor. Up to 12,500 scans were necessary to obtain a well-resolved spectrum.

The density and strength of the acid sites of the different AlSBA-15 materials were determined by temperature-programmed-desorption (TPD) of pyridine. About 100 mg of the materials were evacuated for 3 h at 250 °C under vacuum ($P < 10^{-5}$ hPa). Thereafter, the samples were cooled to room temperature under dry nitrogen followed by exposure to a stream of pyridine in nitrogen for 30 min. Subsequently, the physisorbed pyridine was removed by heating the sample to 120 °C for 2 h in a nitrogen flow. The temperature-programmed desorption (TPD) of pyridine was performed by heating the sample in a nitrogen flow (50 ml/min) from 120 to 600 °C with a rate of 10 K/min using a high-resolution thermogravimetric analyzer coupled with a mass spectrometer (SETARAM setsys 16MS). The observed

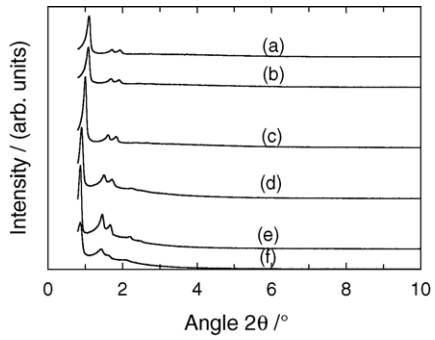

Fig. 1. XRD powder patterns of AlSBA-15 materials prepared with different n_{Si}/n_{Al} ratios: (a) SBA-15, (b) AlSBA-15(215) (c) AlSBA-15(136), (d) AlSBA-15(45), (e) AlSBA-15(12) and (f) AlSBA-15(7).

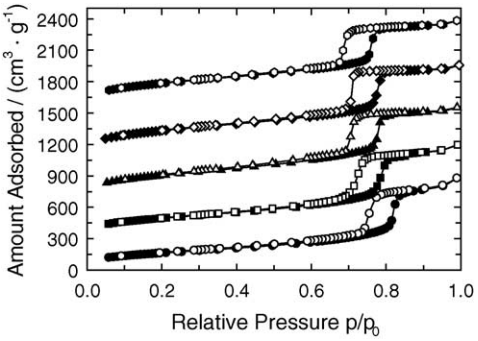

Fig. 2. Nitrogen adsorption isotherms of AlSBA-15 materials prepared with different n_{Si}/n_{Al} ratios (closed symbols, adsorption; open symbols, desorption): (●) AlSBA-15(7), (■) AlSBA-15(12), (▲) AlSBA-15(45), (◆) AlSBA-15(136) and (⬣) AlSBA-15(215).

weight loss was used to quantify the number of acid sites assuming that each mole of pyridine corresponds to one mole of protons.

2.3. Catalytic studies

The *tert*-butylation of phenol was carried out in a fixed-bed flow-type reactor made up of a borosil glass tube with a length of 40 cm and an internal diameter of 2 cm. About 0.5 g of catalyst were placed in the reactor and supported on either side with a thin layer of quartz wool and ceramic beds. The reactor was heated to the reaction temperature with the help of a tubular furnace controlled by a digital temperature controller. The catalyst was activated in air at 500 °C for 6 h prior to the catalytic runs. Reactants were fed into the reactor using a syringe infusion pump. The bottom of the reactor was connected to a coiled condenser and receiver to collect the products. The products obtained in the first 20 min were discarded and the product collected after different time-on-stream was analyzed for identification. The liquid products were analyzed using a Shimadzu gas chromatograph GC-17A using a DB-5 capillary column. Product identification was achieved by co-injection and GC–MS.

3. Results and discussion

The chemical analysis of AlSBA-15 materials synthesized by using aluminum isopropoxide as the Al source with different n_{Si}/n_{Al} ratio is summarized in Table 1. In all cases, the n_{Si}/n_{Al} ratio of the calcined materials is significantly higher than the n_{Si}/n_{Al} ratio in the synthesis gel. This is probably a consequence of the solubility of aluminum isopropoxide in the acidic medium, which allows only statistical replacement of Si by Al. However, AlSBA-15 materials with n_{Si}/n_{Al} ratios ranging from 215 to 7 have been synthesized.

Fig. 1 exhibits the XRD powder patterns of the AlSBA-15 samples synthesized with different n_{Si}/n_{Al} ratios. All samples show four well resolved peaks which are indexed to the (1 0 0), (1 1 0) and (2 0 0) and (2 1 0) reflections of the hexagonal space group p6mn. Interestingly, the line width of the reflections increases with decreasing n_{Si}/n_{Al} ratio except for AlSBA-15(7) which is probably a consequence of the decreasing particle size. For AlSBA-15(7), all reflections are relatively broad.

The nitrogen adsorption isotherms of AlSBA-15 (Fig. 2) are of type IV of the IUPAC classification. All isotherms show a sharp steep rise at a relative pressure of 0.63–0.9, which confirms the presence of large mesopores. The capillary condensation step is shifted to higher relative pressure with increasing aluminum content of the samples. This is attributed to an increase of the pore diameter with rising Al content of the samples. Consequently, specific surface area and specific pore volume of the AlSBA-15 materials also vary with Al content (Table 1). With increasing Al content, the pore diameter increases from 8.9 to 11.8 nm, while the specific surface area decreases

Table 1
Textural properties of AlSBA-15 samples prepared with different n_{Si}/n_{Al} ratios

Sample	a_0 (nm)	n_{Si}/n_{Al} (gel)	n_{Si}/n_{Al} (product)	A_{BET} (m^2/g)	Pore volume (cm^3/g)	Pore diameter $d_{p,ads}$ (nm)
AlSBA-15(7)	11.76	3	7	604	1.26	11.8
AlSBA-15(12)	11.76	5	12	719	1.30	9.7
AlSBA-15(45)	11.27	7	45	930	1.35	9.7
AlSBA-15(136)	10.23	14	136	1026	1.35	9.6
AlSBA-15(215)	9.59	27	215	1033	1.31	8.9
SBA-15	9.28	55	364	1039	1.28	8.9

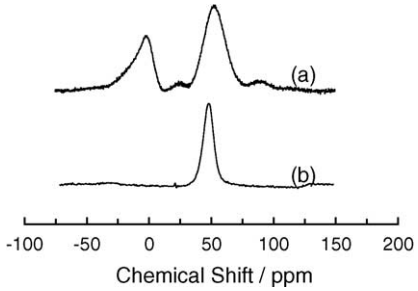

Fig. 3. ^{27}Al MAS NMR spectra of AlSBA-15 materials prepared with different n_{Si}/n_{Al} ratios: (a) AlSBA-15(7) and (b) AlSBA-15(45).

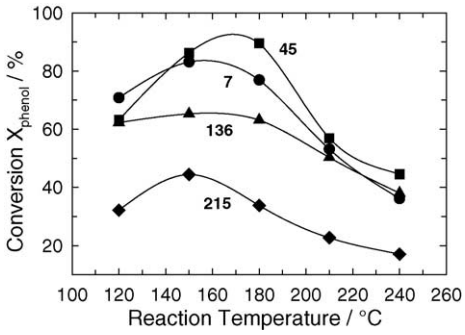

Fig. 4. Effect of temperature on the *tert*-butylation of phenol over AlSBA-15 with different n_{Si}/n_{Al} ratios at a WHSV of 4.90 h^{-1} and $n_{t\text{-butanol}}/n_{phenol}$ = 4: (●) AlSBA-15(7), (■) AlSBA-15(45), (▲)AlSBA-15(136) and (◆) AlSBA-15(215).

from 1040 to 604 m^2/g. For materials having cylindrical pores, the surface area is inversely proportional to the pore diameter of the materials (d_p = 4V/A) and, thus, a decrease of the specific surface area has to be expected. It is interesting to note that both the unit cell parameter a_0 and the pore diameter increase significantly with increasing Al content in the synthesis gel and the final product (Table 1). A similar trend has been found when aluminum isopropoxide is used as the Al source for the synthesis of AlMCM-48 [31]. The mechanism of the observed pore size enlargement is currently not known and subject to further studies.

The ^{27}Al MAS NMR spectra of the calcined AlSBA-15(7) and AlSBA-15(45) are shown in Fig. 3. All samples with n_{Si}/n_{Al} ratio $\geq$ 45 show only one peak at ca. 50 ppm indicative of aluminum in tetrahedral coordination. However, for AlSBA-15(7) one peak centered at ca. 53 ppm and two small peaks centered around 7 and 22 ppm are observed. The peak at 53 ppm is attributed to aluminum in tetrahedral coordination, while the peak at ca. 7 ppm is attributed to octahedrally coordinated aluminum. The peak at 22 ppm might be indicative of Al in five-fold coordination. A similar behavior has been reported for AlMCM-41 [32–37]. A more detailed study of the incorporation of aluminum into SBA-15 is found in our previous paper [15].

The density and the strength of the acid sites were determined using temperature-programmed-desorption (TPD) of pyridine and the data are collected in Table 2. Weak (weight loss between 120 and 350 °C), moderate (350–450 °C) and strong (450–600 °C) acid sites are found in all samples. The weak acid sites are attributed to surface hydroxyl groups and the medium and the strong acid sites originate from the incorporation of aluminum atoms into the SBA-15 walls. It is interesting to note that the number of weak acids sites attributed to weakly held hydrogen-bonded pyridine on terminal silanol group increases with rising n_{Si}/n_{Al} ratio. This is consistent with the fact that the concentration of terminal silanol groups per fixed weight of samples is expected to increase with n_{Si}/n_{Al} ratio. However, the amount of medium acid sites decreases with increasing n_{Si}/n_{Al} ratio. It should be noted that the total number of acid sites (medium and strong acid sites) of AlSBA-15(45) is higher than that of AlSBA-15(7) and AlSBA-15(136). This could be due to the larger number of extra-framework aluminum atoms in AlSBA-15(7). The total number of acid sites increases in the following order: AlSBA-15(45) > AlSBA-15(7) > AlMCM-41(23) > AlSBA-15(136). It has to be pointed out that the determination of the amount of acid sites by pyridine desorption is not straight forward. At temperatures above 450 °C, pyridine might as well desorb from strong Lewis acid sites and water might be formed by dehydroxylation of the Brønsted sites. Spectroscopic studies are underway to address these points.

4. Catalytic activity

Fig. 4 shows the conversion of phenol over AlSBA-15 catalysts with different n_{Si}/n_{Al} ratios as a function of the reaction temperature in the alkylation of phenol with *tert*-butanol at a WHSV of 4.9 h^{-1} and a $n_{t\text{-butanol}}/n_{phenol}$ ratio of 4. The phenol conversions, product yields and selectivities observed over different catalysts are summarized in Table 3. The products obtained are 2-*tert*-butylphenol (2-TBP), 4-*tert*-

Table 2
Density and strength of acid sites of AlSBA-15 catalysts with different n_{Si}/n_{Al} ratios

Catalyst	Acid sites (mmol/g)			
	Weak (120–350 °C)	Medium (351–450 °C)	Strong (>450 °C)	Total (>350 °C)
AlMCM-41(23)	0.754	0.088	0.271	0.359
AlSBA-15(7)	0.241	0.248	0.139	0.386
AlSBA-15(45)	0.418	0.182	0.257	0.438
AlSBA-15(136)	0.471	0.108	0.162	0.270

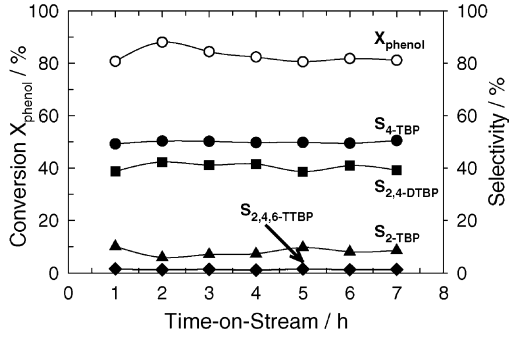

Fig. 5. Effect of time on stream on phenol conversion and product selectivities over AlSBA-15(45) at T_R = 150 °C, WHSV = 5.04 h^{-1}, $n_{t\text{-butanol}}/n_{phenol}$ = 3: (○) X_{phenol}, (●) $S_{4\text{-TBP}}$, (■) $S_{2,4\text{-DTBP}}$, (▲) $S_{2\text{-TBP}}$ and (◆) $S_{2,4,6\text{-TTBP}}$.

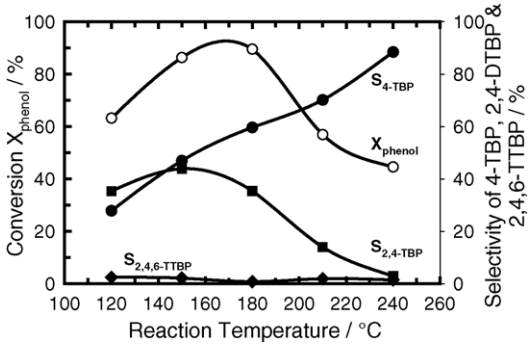

Fig. 6. Effect of temperature on phenol conversion and product selectivities over AlSBA-15(45) at WHSV 4.90 h^{-1}, $n_{t\text{-butanol}}/n_{phenol}$ = 4, time-on-stream = 2 h: (○) X_{phenol}, (●) $S_{4\text{-TBP}}$, (■) $S_{2,4\text{-DTBP}}$, (▲) $S_{2\text{-TBP}}$ and (◆) $S_{2,4,6\text{-TTBP}}$.

butyl phenol (4-TBP) and 2,4 di-*tert*-butylphenol (2,4-DTBP). Only a small quantity of 2,4,6-tri-*tert*-butylphenol (2,4,6-TTBP) was observed, while the formation of 3-*tert*-butyl phenol (3-TBP) was not observed. At low reaction temperatures, 2-TBP and 2,4-di-*tert*-butylphenol (2,4-DTBP) are predominantly formed, while 4-TBP is the major product at $T \geq 150$ °C. A phenol conversion of 89.5% was observed for AlSBA-15(45) at a reaction temperature of 180 °C, which is higher as compared to other catalysts such as AlMCM-41, FeMCM-41 and FeAlMCM-41 under comparable conditions. Concerning the distribution of the reaction products, it is interesting to note that a significantly higher selectivity for the dialkylated products (ca. 40%) is observed for all AlSBA-15 catalysts as compared to other mesoporous materials. A selectivity of only 4% for the dialkylated product was observed over AlMCM-41 under comparable conditions [27]. For AlSBA-15(45) the 4-TBP yield amounts to 40.5% and the 2,4-DTBP yield corresponds to 37.9% (T_R = 150 °C). The relatively large amount of 2,4-DTBP indicates that the AlSBA-15(45) catalyst possesses a higher number of medium or strong acid sites as compared to other mesoporous materials (Table 2). The activity of the catalysts employed in this study declines in the following order: AlSBA-15(45) > AlSBA-15(7) > AlSBA-15(136) > AlSBA-15(215). Although AlSBA-15(7) has a lower n_{Si}/n_{Al} ratio, the conversion of phenol over this catalyst is lower as compared with AlSBA-15(45). This is probably due to the higher number of extra framework aluminums atoms in AlSBA-15(7) (Fig. 3). As AlSBA-15(45) has demonstrated superior activity in *tert*-butylation of phenol under the prevailing reaction conditions, detailed catalytic studies including viz., time-on-stream behavior, effects of temperature, WHSV and feed ratio on the conversion and product yield have been carried out only with this catalyst.

Fig. 5 shows phenol conversion and selectivity to alkylated products over AlSBA-15(45) as a function of time-on-stream at a reaction temperature of 150 °C, a WHSV of 5.04 h^{-1} and a $n_{t\text{-butanol}}/n_{phenol}$ ratio of 3. After two hours on stream, the phenol conversion amounts ca. 88%. The product selectivities to 4-TBP and 2,4-DTBP amount to 47.0 and 43.9%, respectively, and do not change significantly with time-on-stream. However, the conversion drops to 81% within 7 h of reaction, indicating only a slight deactivation of the catalyst probably due to coking. The selectivity for the alkylated products does not change with time-on-stream indicating that secondary reactions such as dealkylation and transalkylation do not occur to significant extent over this catalyst. Moreover, the yield of oligomerized

Table 3
tert-Butylation of phenol over AlSBA-15 catalysts (reaction conditions: T_R = 150 °C, $n_{t\text{-butanol}}/n_{phenol}$ = 4, WHSV = 4.90 h^{-1}, time-on-stream = 2 h)

Catalyst	AlSBA-15(7)	AlSBA-15(45)	AlSBA-15(136)	AlSBA-15(215)
Product yield (%)				
2-TBP	7.5	6.0	14.0	6.8
4-TBP	39.3	40.5	25.9	19.2
2,4-DTBP	34.6	37.9	21.9	11.4
2,4,6-TTBP	1.5	1.9	1.1	0
Phenyl-*tert*-butyl ether	–	-	2.1	7.0
Others	0.3	0.0	0.3	0.1
X_{Phenol} (%)	83.2	86.3	65.3	44.5
Selectivity (%)				
2-TBP	9.1	7.0	21.5	15.3
4-TBP	47.3	47.0	39.7	43.2
2,4-DTBP	41.7	43.9	33.6	25.7
2,4,6-TTBP	1.8	2.1	1.8	0

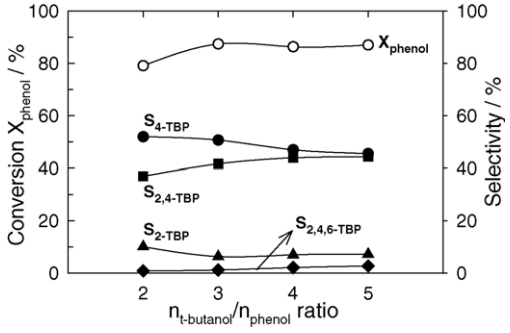

Fig. 7. Effect of $n_{t\text{-butanol}}/n_{phenol}$ ratio on the activity and selectivity of AlSBA-15(45) at 150 °C, WHSV 4.90 h^{-1}, time-on-stream = 2 h: (○) X_{phenol}, (●) $S_{4\text{-TBP}}$, (■) $S_{2,4\text{-DTBP}}$, (▲) $S_{2\text{-TBP}}$ and (◆) $S_{2,4,6\text{-TTBP}}$.

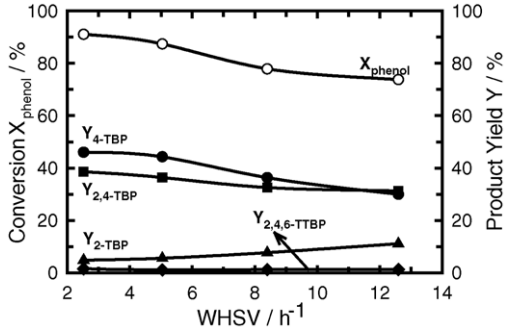

Fig. 8. Influence of WHSV on phenol conversion and product distribution over AlSBA-15(45) (T_R = 150 °C, $n_{t\text{-butanol}}/n_{phenol}$ = 3, time-on-stream = 2 h: (○) X_{phenol}, (●) $Y_{4\text{-TBP}}$, (■) $Y_{2,4\text{-DTBP}}$, (▲) $Y_{2\text{-TBP}}$ and (◆) $Y_{2,4,6\text{-TTBP}}$.

products ($Y < 0.3\%$) is almost constant with time-on-stream. When compared with other mesoporous materials such as FeMCM-41, AlMCM-41 and FeAlMCM-41 [27,28,30], the deactivation rate of AlSBA-15(45) is lower. This behavior is tentatively assigned to its larger pore size compared to other mesoporous materials and/or higher number of strong acid sites.

Over AlSBA-15(45), the conversion of phenol increases from 63.2 to 89.5% with increasing reaction temperature from 120 to 180 °C and then decreases to 44.6% at 240 °C (Fig. 6 and Table 4). This behavior is often observed in alkylation reactions and is mainly due to the thermodynamics of alkylation and dealkylation. Moreover, the olefins produced by dehydration of *tert*-butanol are probably consumed in more than one parallel reaction such as alkylation, oligomerization and cracking. It is well known that oligomerization and cracking are dominant at high reaction temperatures, which results in a reduced phenol conversion at higher temperature even in excess of the alkylation agent. The results obtained in this study are in good agreement with those reported by Liu et al. [38] for the *tert*-butylation of naphthalene. In addition, at higher temperatures dealkylation of the formed butyl phenols becomes more dominant. The selectivity for 4-TBP increases monotonously from 27.8 to 88.4% with increasing reaction temperature whereas the selectivity of 2-TBP decreases from 30.1 to 7.2%. It has been suggested that 2-TBP is initially formed and subsequently isomerized to 4-TBP, which is in line with our observations. The selectivity for 2,4-DTBP increases from 35.4 to 43.9% by raising the reaction temperature from 120 to 150 °C and then declines to 2.9% at a reaction temperature of 240 °C. In addition to an increased dealkylation rate at higher temperature, it is also possible that some of the strong acid sites may be blocked by coke, which suppresses the formation of dialkylated products, which require strong acid sites for their formation. Moreover, the formation of undesired products such as oligomerized products (C_8 or C_{12}) may consume *tert*-butanol without yielding dialkylated products such as 2,4-DTBP [25]. The above results show that moderate reaction temperatures (120–150 °C) are required to enhance the selectivity for the formation of 2,4-DTBP.

With increasing molar $n_{t\text{-butanol}}/n_{phenol}$ ratio from 2 to 5, the conversion of phenol increases from 79 to 87% (Fig. 7). It was reported earlier [21,22,39] that polar molecules such as methanol and higher alcohols compete with phenol for adsorption sites and thus phenol conversion initially rises with increasing amount of alkylating agent as observed in the present study. In addition, the selectivity to 2,4-DTBP and 2,4,6-TTBP increases with increasing amount of *tert*-butanol in the feed at the expense of the monoalkylated products 4-TBP and 2-TBP. The increase in the selectivity for the higher-alkylated products 2,4-DTBP and 2,4,6-TTBP is probably due to the increased availability of *tert*-butanol molecules in the reactant feed. Similar result has been reported for AlMCM-41 [27,30] and microporous aluminophosphates [40].

The reaction was also carried out at 150 °C and a constant $n_{t\text{-butanol}}/n_{phenol}$ ratio of 3 at different WHSV (Fig. 8). Phenol conversion decreases with higher space velocity, which is

Table 4
Effect of temperature on *tert*-butylation of phenol over AlSBA-15(45) at $n_{t\text{-butanol}}/n_{phenol}$ = 4; WHSV = 4.90 h^{-1}; time-on-stream = 2 h

Temperature (°C)	Conversion X_{phenol} (%)	$S_{product}$ (%)				$Y_{product}$ (%)			
		2-TBP	4-TBP	2,4-DTBP	2,4,6-TTBP	2-TBP	4-TBP	2,4-DTBP	2,4,6-TTBP
120	63.2	30.1	27.8	35.4	2.5	19.0	17.6	22.3	1.6
150	86.3	7.0	47.0	43.9	2.1	6.0	40.5	37.9	1.9
180	89.5	3.9	59.6	35.4	0.8	3.5	53.4	31.7	0.7
210	56.9	12.7	70.2	14.0	2	7.3	39.9	8.0	1.1
240	44.6	7.2	88.4	2.9	1.5	3.2	39.4	1.3	0.7

due to the reduced contact time. The yield of 2-TBP increases with increasing WHSV whereas the yields of 4-TBP, 2,4-DTBP and 2,4,6-TTBP decrease. The increase of the 2-TBP yield with increasing space velocity has been ascribed to the elimination of interparticle diffusional resistances at higher space velocities [27], but might as well indicate that this product is formed initially and later converted to the secondary products such as 4-TBP and 2,4-DTBP.

5. Conclusions

In the present study, the mesoporous molecular sieve AlSBA-15 has been synthesized with n_{Si}/n_{Al} ratios between 7 and 215. XRD and N_2 adsorption measurements of the obtained AlSBA-15 materials confirm that the structure of the materials is maintained even at low n_{Si}/n_{Al} ratio. The textural properties are changed with the increasing aluminum loading. In particular, the pore diameter increases from 8.9 ($n_{Si}/n_{Al} = 215$) to 11.8 ($n_{Si}/n_{Al} = 7$) nm. The ^{27}Al MAS NMR spectra confirm that aluminum is exclusively in tetrahedral coordination (except for AlSBA-15(7), where also octahedrally-coordinated aluminum is observed) forming Brønsted acid sites. The catalytic activity of the AlSBA-15 samples was tested in the acid-catalyzed vapor phase tertiary-butylation of phenol employing *tert*-butanol as the alkylation agent. Among all catalyst used, AlSBA-15(45) was the most active, showing a high phenol conversion ($X = 82.3\%$) and high yields of 4-TBP ($S = 40.5\%$) and 2,4-DTBP ($S = 37.9\%$) at a reaction temperature of 150 °C. The formation of a large amount of the dialkylated product 2,4-DTBP is observed at low reaction temperatures giving additional evidence for the presence of strong acid sites in AlSBA-15 formed by the incorporation of aluminum into the amorphous walls. Moreover, the conversion of phenol and the selectivity to 4-TBP and 2,4-DTBP observed over the novel catalysts are significantly higher as compared to FeAlMCM-41, AlMCM-41, FeMCM-41 or FeSBA-1 reported earlier.

Acknowledgements

Financial support of the work by DAAD and DST is gratefully acknowledged. M.H. thanks Fonds der Chemischen Industrie for generous support.

References

[1] J.S. Beck, J.C. Vartuli, W.J. Roth, M.E. Leonowicz, C.T. Kresge, K.T. Schmitt, C.T. Chen, D.H. Olson, E.W. Sheppard, S.B. McCullen, J.B. Higgins, J.L. Schlenker, J. Am. Chem. Soc. 114 (1992) 10834.
[2] J.F. Diaz, K.J. Balkus, J. Mol. Catal. B: Enzym. 2 (1996) 115.
[3] Z. Luan, H. He, W. Zhou, C.-F. Cheng, J. Klinowski, J. Chem. Soc., Faraday Trans. 91 (1995) 2955.
[4] Z. Luan, C.-F. Cheng, H. He, J. Klinowski, J. Phys. Chem. 99 (1995) 10590.
[5] D. Zhao, Q. Huo, J. Feng, B.F. Chmelka, G.D. Stucky, J. Am. Chem. Soc. 120 (1998) 6024.
[6] P. Yang, D. Zhao, D. Margolese, B.F. Chmelka, G.D. Stucky, Nature 396 (1998) 152.
[7] P. Yang, D. Zhao, D. Margolese, B.F. Chmelka, G.D. Stucky, Chem. Mater. 11 (1999) 2831.
[8] (a) Y. Yue, A. Gédéon, J.-L. Bonardet, N. Melosh, J.-B. D'Espinose, J. Fraissard, Chem. Commun. (19991967);
(b) A. Gedeon, A. Lassoued, J.L. Bonardet, J. Fraissard, Microporous Mesoporous Mater. 44–45 (2001) 801.
[9] Z. Luan, M. Hartmann, D. Zhao, W. Zhou, L. Kevan, Chem. Mater. 11 (1999) 1621.
[10] W.-H. Zhang, J. Lu, B. Han, M. Li, J. Xiu, P. Ying, C. Li, Chem. Mater. 14 (2002) 3413.
[11] M. Cheng, Z. Wang, K. Sakurai, F. Kumata, T. Saito, T. Komatsu, T. Yashima, Chem. Lett. (1999) 131.
[12] Z. Luan, E.M. Maes, P.A.W. van der Heide, D. Zhao, R.S. Czernuszewicz, L. Kevan, Chem. Mater. 11 (1999) 3680.
[13] Z. Luan, J.Y. Bae, L. Kevan, Chem. Mater. 12 (2000) 3202.
[14] R. Murugavel, H.W. Roesky, Angew. Chem. Int. Ed. Engl. 109 (1997) 4491.
[15] A. Vinu, V. Murugesan, W. Böhlmann, M. Hartmann, J. Phys. Chem. B. 108 (2004) 11496.
[16] A. Knop, L.A. Pilato, Phenolic Resin Chemistry, Springer, Berlin, 1985.
[17] J.B. Niederl, S. Natelson, J. Am. Chem. Soc. 53 (1938) 272.
[18] K.G. Chandra, M.M. Sharma, Catal. Lett. 19 (1993) 309.
[19] R.A. Rajadhyaksha, D.D. Chaudhari, Ind. Eng. Chem. Res. 26 (1987) 1276.
[20] S. Namba, T. Yashima, Y. Itaba, N. Hara, Stud. Surf. Sci. Catal. 5 (1980) 105.
[21] R.F. Parton, J.M. Jacobs, D.R. Huybrechts, P.A. Jacobs, Stud. Surf. Sci. Catal. 46 (1989) 163.
[22] R.F. Parton, J.M. Jacobs, H.V. Ootehem, P.A. Jacobs, Stud. Surf. Sci. Catal. 46 (1989) 211.
[23] A. Corma, H. Garcia, J. Primo, J. Chem. Res., Synop. 1 (1998) 40.
[24] K. Zhang, C. Huang, H. Zhang, S. Xiang, S. Liu, D. Xu, H. Li, Appl. Catal. 166 (1998) 89.
[25] K. Zhang, H. Zhang, G. Xu, S. Xiang, D. Xu, S. Liu, H. Li, Appl. Catal. 207 (2001) 183.
[26] N.S. Chang, C.C. Chen, S.J. Chu, P.Y. Chen, T.K. Chuang, Stud. Surf. Sci. Catal. 46 (1989) 223.
[27] A. Sakthivel, S.K. Badamali, P. Selvam, Microporous Mesoporous Mater. 39 (2000) 457.
[28] S.K. Badamali, A. Sakthivel, P. Selvam, Catal. Lett. 65 (2000) 153.
[29] A. Sakthivel, N. Saritha, P. Selvam, Catal. Lett. 72 (2001) 225.
[30] (a) A. Vinu, K. Usha Nandhini, V. Murugesan, W. Böhlmann, V. Umamaheswari, A. Pöppl, M. Hartmann, Appl. Catal. A: Gen. 265 (2004) 1;
(b) A. Vinu, T. Kritiga, V. Murugesan, M. Hartmann, Adv. Mater. 16 (2004) 1817.
[31] C. Bischof, Ph.D. thesis, University of Kaiserslautern (2001).
[32] M. Janicke, D. Kumar, G.D. Stucky, B.F. Chemlka, Stud. Surf. Sci. Catal. 84 (1994) 243.
[33] R.B. Borade, A. Clearfield, Catal. Lett. 31 (1995) 267.
[34] Z. Luan, H. He, C.F. Cheng, W. Zhou, J. Klinowski, J. Phys. Chem. B 99 (1995) 1018.
[35] K.M. Reddy, C. Song, Catal. Lett. 36 (1996) 103.
[36] S. Biz, M.L. Occelli, Catal. Rev. Sci. Eng. 40 (1998) 329.
[37] K.M. Reddy, C. Song, Catal. Today 31 (1996) 197.
[38] Z. Liu, P. Moreau, F. Fajula, Appl. Catal. A. Gen. 159 (1997) 305.
[39] S. Subramanian, A. Mitra, C.V.V. Satyanarayana, D.K. Chakrabarty, Appl. Catal. A Gen. 159 (1997) 229.
[40] C.V. Satyanarayana, U. Sridevi, B.S. Rao, Stud. Surf. Sci. Catal. 135 (2001) 236.